The soft tissue and skeletal anatomy of two Late Jurassic ichthyosaur specimens from the Solnhofen archipelago (#68124)

First submission

Guidance from your Editor

Please submit by **1 Jan 2022** for the benefit of the authors (and your $200 publishing discount) .

Structure and Criteria
Please read the 'Structure and Criteria' page for general guidance.

Author notes
Have you read the author notes on the guidance page?

Raw data check
Review the raw data.

Image check
Check that figures and images have not been inappropriately manipulated.

Privacy reminder: If uploading an annotated PDF, remove identifiable information to remain anonymous.

Files
Download and review all files from the materials page.

7 Figure file(s)
1 Other file(s)

Structure and Criteria

Structure your review

The review form is divided into 5 sections. Please consider these when composing your review:

1. **BASIC REPORTING**
2. **EXPERIMENTAL DESIGN**
3. **VALIDITY OF THE FINDINGS**
4. General comments
5. Confidential notes to the editor

You can also annotate this PDF and upload it as part of your review

When ready submit online.

Editorial Criteria

Use these criteria points to structure your review. The full detailed editorial criteria is on your guidance page.

BASIC REPORTING

- Clear, unambiguous, professional English language used throughout.
- Intro & background to show context. Literature well referenced & relevant.
- Structure conforms to PeerJ standards, discipline norm, or improved for clarity.
- Figures are relevant, high quality, well labelled & described.
- Raw data supplied (see PeerJ policy).

EXPERIMENTAL DESIGN

- Original primary research within Scope of the journal.
- Research question well defined, relevant & meaningful. It is stated how the research fills an identified knowledge gap.
- Rigorous investigation performed to a high technical & ethical standard.
- Methods described with sufficient detail & information to replicate.

VALIDITY OF THE FINDINGS

- Impact and novelty not assessed. *Meaningful* replication encouraged where rationale & benefit to literature is clearly stated.
- All underlying data have been provided; they are robust, statistically sound, & controlled.
- Conclusions are well stated, linked to original research question & limited to supporting results.

Standout reviewing tips

The best reviewers use these techniques

Tip	*Example*
Support criticisms with evidence from the text or from other sources	*Smith et al (J of Methodology, 2005, V3, pp 123) have shown that the analysis you use in Lines 241-250 is not the most appropriate for this situation. Please explain why you used this method.*
Give specific suggestions on how to improve the manuscript	*Your introduction needs more detail. I suggest that you improve the description at lines 57- 86 to provide more justification for your study (specifically, you should expand upon the knowledge gap being filled).*
Comment on language and grammar issues	*The English language should be improved to ensure that an international audience can clearly understand your text. Some examples where the language could be improved include lines 23, 77, 121, 128 – the current phrasing makes comprehension difficult. I suggest you have a colleague who is proficient in English and familiar with the subject matter review your manuscript, or contact a professional editing service.*
Organize by importance of the issues, and number your points	*1. Your most important issue* *2. The next most important item* *3. …* *4. The least important points*
Please provide constructive criticism, and avoid personal opinions	*I thank you for providing the raw data, however your supplemental files need more descriptive metadata identifiers to be useful to future readers. Although your results are compelling, the data analysis should be improved in the following ways: AA, BB, CC*
Comment on strengths (as well as weaknesses) of the manuscript	*I commend the authors for their extensive data set, compiled over many years of detailed fieldwork. In addition, the manuscript is clearly written in professional, unambiguous language. If there is a weakness, it is in the statistical analysis (as I have noted above) which should be improved upon before Acceptance.*

The soft tissue and skeletal anatomy of two Late Jurassic ichthyosaur specimens from the Solnhofen archipelago

Lene L Delsett [Corresp., 1, 2], **Henrik Friis** [3], **Martina Kölbl-Ebert** [4], **Jørn Hurum** [3]

[1] Department of Paleobiology, National Museum of Natural History, Smithsonian Institution, Washington DC, District of Columbia, United States of America

[2] Centre for Ecological and Evolutionary Synthesis, University of Oslo, Oslo, Norway

[3] Natural History Museum, University of Oslo, Oslo, Norway

[4] Department of Earth and Environmental Sciences, Ludwig Maximilian Universität, Munich, Germany

Corresponding Author: Lene L Delsett
Email address: DelsettL@si.edu

Ichthyosaurs from the Solnhofen Lagerstätte are among the only examples of soft tissue preservation in the major Middle Jurassic – middle Cretaceous family Ophthalmosauridae. However, few such specimens are currently described, and the taphonomical pathways for the preservation of soft tissue are not well understood. In order to answer this, two new ichthyosaur specimens, one nearly complete and one isolated tail, are described here. The nearly complete specimen is assigned to *Aegirosaurus* sp. It is accompanied by large amounts of incrustation pseudomorphs (epimorphs) of soft tissue preserved as apatite. It also preserves a nearly complete gastral basket, for the first time in ophthalmosaurids. Soft tissue samples were analyzed using X-ray diffraction (XRD) and scanning electron microscopy (SEM) coupled with energy dispersive spectroscopy (EDS) analysis. The analyses confirm the presence of apatite, with phosphate most likely derived from the body itself.

The soft tissue and skeletal anatomy of two Late Jurassic ichthyosaur specimens from the Solnhofen archipelago

Lene Liebe Delsett[12], Henrik Friis[3], Martina Kölbl-Ebert[4], Jørn Harald Hurum[3]

[1]Department of Paleobiology, National Museum of Natural History, Smithsonian Institution, 10th St. & Constitution Ave. NW Washington, D.C. 20560, United States of America

[2]Centre for Ecological and Evolutionary Synthesis, University of Oslo, P.O. Box 1066 Blindern, 0316 Oslo, Norway

[3]Natural History Museum, University of Oslo, P.O. Box 1172 Blindern, 0318 Oslo, Norway

[4]Department of Earth and Environmental Sciences, Ludwig Maximilian Universität, Luisenstraße 37, 80333 Munich, Germany

Corresponding Author:
Lene Liebe Delsett[12]
10th St. & Constitution Ave. NW Washington, D.C. 20560, United States of America

Email address: DelsettL@si.edu

Abstract

Ichthyosaurs from the Solnhofen Lagerstätte are among the only examples of soft tissue preservation in the major Middle Jurassic – middle Cretaceous family Ophthalmosauridae. However, few such specimens are currently described, and the taphonomical pathways for the preservation of soft tissue are not well understood. In order to answer this, two new ichthyosaur specimens, one nearly complete and one isolated tail, are described here. The nearly complete specimen is assigned to *Aegirosaurus* sp. It is accompanied by large amounts of incrustation pseudomorphs (epimorphs) of soft tissue preserved as apatite. It also preserves a nearly complete gastral basket, for the first time in ophthalmosaurids. Soft tissue samples were analyzed using X-ray diffraction (XRD) and scanning electron microscopy (SEM) coupled with energy dispersive spectroscopy (EDS) analysis. The analyses confirm the presence of apatite, with phosphate most likely derived from the body itself.

Introduction

Ichthyosaurs were marine pursuit predators that lived from the Early Triassic to the middle Cretaceous (Fischer et al. 2016). Their rich fossil record of skeletal elements and teeth are ideal for analyses of ecological interactions and evolutionary patterns in the marine realm (spanning approx. ~~150~~ million years), and display many examples of convergent evolution to cetaceans, e.g. in body shape and swimming performance (Cozzi et al. 2017; Lindgren et al. 2018). To fully understand their adaptations, fossilized soft tissue is crucial, but presently, the nature and diagenetic processes affecting soft tissue preservation in ichthyosaurs are not well understood (Lindgren et al. 2018).

Soft tissue in ichthyosaur fossils has been observed for almost two centuries (Fraas 1888; Lydekker 1889; Martill 1987; Martill 1995; Martin et al. 1986; e. g. Owen 1841; Whitear 1956), see summary in Martill (1993). The vast majority are specimens from the Lower Jurassic (Hettangian to Toarcian) and some from the Middle Jurassic (Callovian) of Europe. The most famous of these are *Stenopterygius* specimens from the Toarcian Posidonia Shale of Holzmaden in Baden Württenburg, Germany. Preserved body outlines show that ichthyosaurs had a dorsal fin, a vertically oriented caudal fin and external hind limbs (Böttcher 1990; Huene 1922; Lindgren et al. 2018; Martill 1993; Maxwell 2012a; Maxwell 2012b; Renesto et al. 2020). Recent studies have revealed the structure and color of ichthyosaur skin in a few key specimens from the Early Jurassic and shown that some ichthyosaurs had blubber (Lindgren et al. 2014; Lindgren et al. 2018). However, for later ichthyosaurs (Middle Jurassic-Cretaceous), records of soft tissue are very few, including an *Ophthalmosaurus* specimen from the Middle Jurassic of England (Martill 1987), a *Maiaspondylus* specimen from the Lower Cretaceous of Canada (Maxwell & Caldwell 2006) and ichthyosaurs from the Solnhofen Plattenkalk.

The Solnhofen Plattenkalk (Fig. 1) is a Late Jurassic *Konservat-Lagerstätte* preserving many vertebrates and invertebrates with soft tissue, most famously *Archaeopteryx lithographica* (Rauhut et al. 2018). Ichthyosaur fossils were first found in the Solnhofen deposits in 1852, but are uncommon (Bardet & Fernández 2000; Barthel et al. 1990; Meyer 1863; Wagner 1853). Examples of Solnhofen ichthyosaurs with preserved soft tissue have been described by Bauer (1898), and in two specimens of *Aegirosaurus leptospondylus* (Bardet & Fernández 2000).

Here we describe two ichthyosaur specimens with soft tissue from the Solnhofen area from the collection of Bishops Seminar Eichstätt, housed in the Jura-Museum Eichstätt (Figs. 2-3). JME-SOS-08369 is a nearly complete skeleton that was recently excavated and prepared, whereas JME-SOS2183 is a tail that was discovered in 1926. None of them have been formally described previously. In addition, we provide a first analysis of the phosphatized soft tissue in the nearly complete specimen. Phosphatization of soft tissue is common in Solnhofen, and fluorapatite, especially in the form of francolite, typical for preservation of muscle fibers (Barthel et al. 1990). The phosphorus (P) is commonly interpreted to originate from an external source (Wilby & Briggs 1997), but in this contribution, we discuss whether it could instead be derived from the body of the animal itself. As previous studies on ophthalmosaurid specimens with soft tissue were only executed using regular light without mineralogical or elemental analyses (Bardet & Fernández 2000; Maxwell & Caldwell 2006), this is the first geochemical and UV analysis for this clade.

The apatite supergroup of minerals contains more than 40 different mineral species, but all have the same basic crystal structure. The flexibility of the apatite structure means that it can incorporate many elements into the general formula $M1_2M2_3(TO_4)_3X$; where M are large cations, like Ca^{2+}, $Sr^{2+,}$ Pb^{2+}, Ce^{3+}, Na^{1+}; T are high valance cations like P^{5+}, As^{5+}, V^{5+}, Si^{4+}, S^{6+} and X are anions like F^-, Cl^-, $(OH)^-$ or O^{2-}. Hydroxylapatite, ideally $Ca_5(PO_4)_3(OH)$, is the mineral forming bones and teeth. Although mineral formulas are often given as ideal endmembers, like above, apatite typically incorporates other elements in significant amounts, without resulting in formation of a new mineral species. The substitution mechanisms can be homovalent, e. g. F^- substituting $(OH)^-$, or heterovalent. To maintain the overall charge of the structure, the

heterovalent substitutions typically involves multiple sites in the structure, which is known as coupled substitution. Typical examples of coupled substitutions in apatite are: $Ce^{3+} + Na^{+} \leftrightarrow 2Ca^{2+}$; $Ce^{3+} + O^{2-} \leftrightarrow Ca^{2+} + F^{-}$ or $S^{6+} + Na^{1+} \leftrightarrow P^{5+} + Ca^{2+}$. For a review of chemical variation and substitution mechanisms in apatite see Pan and Fleet (2002). The term francolite is often used for sedimentary calcium phosphate, but is not a valid mineral species name, rather a carbonate-rich apatite with a varied composition between fluorapatite and hydroxylapatite (Knudsen & Gunter 2002; McArthur 1985; Pasero et al. 2010). Despite not being a valid mineral species, we prefer to use the term francolite here for consistency with other papers in the field.

Geological setting

The ichthyosaur specimens examined here originate from the locality Eichstätt-Blumenberg of Bavaria, southeastern Germany. The strata are the early Tithonian (Late Jurassic) Eichstätt Plattenkalk, of the Kimmeridgian to early Tithonian Solnhofen Archipelago (Fig. 1). At the time of deposition, the area was situated around 34 degrees north (Munnecke et al. 2008), at the northern margin of the Tethys Ocean. The Plattenkalk deposits are carbonate successions of finely laminated limestone deposited in a series of subtropical, shallow to deeper basins within a huge carbonate platform (Kölbl-Ebert et al. 2005). The carbonate platform was formed largely by sponge-microbial reefs and accumulated carbonate sands, and locally by small coral reefs (Koch et al. 1994; Munnecke et al. 2008). The bottom waters of the basins within the platform were occasionally stagnant, and in some cases possibly characterized by an elevated salinity and microbial films leading to Plattenkalk deposition, which might be the cause of the excellent fossil preservation (Barthel 1970; Gäb et al. 2020; Munnecke et al. 2008).

Materials & Methods

The nearly complete ichthyosaur skeleton (JME-SOS-08369) (Fig. 2) was excavated in 2009 and prepared at the Jura-Museum Eichstätt (Radecker 2014). It was preserved on four slabs and prepared from the field-up side, exposing the specimen in oblique view, showing partly the ventral, partly the right-lateral side. Because a major part of the preparation was done under ultraviolet (UV) light to see details, non-fluorescent and UV stable glue and hardener were used (polyvinylbutyral and a non-reflecting hardener), except on the tail slab, where epoxy was used (Radecker 2014). For a discussion of use of UV in observing fossils in lithographic limestones see Haug et al. (2009).

The second specimen (JME-SOS2183) (Fig. 3) is an ichthyosaur tail with a soft tissue outline, preserved in lateral view. It was found by Karl W. (last name not known) in Blumenberg in 1926 and has at some point been stabilized by paraloid or an equivalent consolidant (Christina Ifrim, pers. comm.). It was pictured, but not formally described, by Martill (1993).

The skeletal descriptions and measurements are based on personal inspection by LLD, JHH and MKE in 2017. The specimens were photographed while mounted, in exhibition light, in low angle regular light, and in UV light, with a Fujifilm x100F camera (ISO 800 – aperture 1/8). A hand-held lamp produced low angle light illumination, and a UV lamp with a wavelength 366 nm was used. Observations derived during the preparation process were contributed by Andreas Radecker (Radecker 2014; pers. comm.). Skeletal comparisons to *Aegirosaurus leptospondylus*

145 are based on personal inspection of a referred specimen (SNSB-BSPG 1954 I 608) by LLD (May
146 2015). The neotype of *Aegirosaurus leptospondylus* was not available for study.
147
148 The nearly complete specimen JME-SOS-08369 preserves fossilized soft tissue of several types.
149 Three samples (JME-SOS-08369-B1, -B2 and -B3, Fig. 4), from the anterior portion of the tail
150 and the surrounding sedimentary matrix were set aside during preparation, and form the basis for
151 this first investigation of the soft tissue. To assess the nature of the soft tissue, XRD and SEM -
152 EDS analyses were performed on the untreated samples of soft tissue. For the XRD analyses,
153 small fragments (max diameter 100-200 μm) were removed from the three samples and mounted
154 with oil in a cryoloop. The analyses were performed in Gandolfi-mode on a Rigaku Synergy-S
155 diffractometer housed at the Natural History Museum in Oslo, using CuKα-radiation (50 kV and
156 1 mA). Diffraction data were collected and processed using the CrysAlisPro software, and
157 diagram matching was performed with Bruker's EVA program with PDF-4 as the database.
158 Based on the XRD analyses, two samples (JME-SOS-08369-B1 and -B2) were chosen for
159 detailed semi-quantitative elemental analyses because they contain apatite in addition to matrix,
160 whereas the third sample (JME-SOS-08369-B3) only contains matrix. The analyses were
161 executed with a Hitachi S-3600N SEM equipped with a Bruker XFlash 5030 energy dispersive
162 detector (EDS), and performed directly on uncoated samples under low vacuum (~10 Pa) with an
163 acceleration voltage of 15 kV and 15 mm working distance. In addition to point analyses,
164 element distribution maps were generated for selected areas of interest. To evaluate the
165 possibility of soft tissue as the phosphorous source for phosphatization, a mass balance was
166 performed. Its constraints were based on cetaceans with similar body shape and size as JME-
167 SOS-08369. For more detailed description of the protocol, see Supplementary materials. Soft

tissue samples from the isolated tail specimen JME-SOS2183 were not analyzed in the present study.

Results

Systematic paleontology

Ichthyosauria de Blainville, 1835

Parvipelvia Motani, 1999

Thunnosauria Motani, 1999

Ophthalmosauridae Baur, 1887

Aegirosaurus Bardet and Fernández, 2000

Aegirosaurus sp.

Referred specimen: Nearly complete skeleton JME-SOS-08369 (Figs. 2, 5, 6, Table S1). The specimen is housed in the Jura-Museum Eichstätt, Eichstätt, Germany.

Locality: The visitor quarry in Eichstätt-Blumenberg.

Age: Early Tithonian (*eigeltingense* horizon), Late Jurassic.

Taxonomic assignment

The nearly complete specimen JME-SOS-08369 can be referred to Ophthalmosauridae with confidence, based on the extensive lateral exposure of the angular (Fernández & Campos 2015; Moon 2017). When compared to *Aegirosaurus leptospondylus*, JME-SOS-08369 shares a snout not markedly demarcated from the skull, delicate and small, densely packed teeth strongly anchored in a dental groove, an enamel crown that is minutely ridged or smooth, a medium sized

orbit, a jugal extending anteriorly to the orbit, and a long and very slender rostrum (Bardet & Fernández 2000). The skull and total body length fall within the original description of the species (Bardet & Fernández 2000). However, the status for more than half of the diagnostic characters cannot be accessed in JME-SOS-08369, including the shape and size of the naris, orbit and sclerotic plates, traits in the postorbital/~~cheek~~ region, as well as all diagnostic postcranial characters. JME-SOS-08369 differs from *Aegirosaurus leptospondylus* in one aspect: it has a maxilla with relatively long lateral exposure, whereas in *Aegirosaurus leptospondylus* the exposure is small (Bardet & Fernández 2000) (pers. observ. LLD SNSB-BSPG 1954 I 608). In conclusion, we refer JME-SOS-08369 to *Aegirosaurus* sp.

Description and comparison of JME-SOS-08369

The specimen (Fig. 2) is articulated and preserved in its entire length, missing only the dorsal portion of the caudal fin. Its total length as preserved is 161 cm from the tip of the snout to the tip of the ventral caudal fin lobe measured in a straight line. During or after death, the animal landed dorsolaterally on the sea floor. Preservation of the skeletal elements is rather poor. The skull (Fig. 5) is compressed, and is seen from the right side. Its total anteroposterior length is 440 mm. The jaw consists of the ~~tooth-bearing~~ right premaxilla and maxilla seen in lateral view, as well as the right dentary, surangular, splenial, and angular. The posterior portion of the left lower jaw elements are preserved and seen in medial view. Anterior to the orbit and in the posteriormost portion, the skull has suffered considerable distortions. The preserved soft tissue is described below.

Premaxilla

The premaxilla is slender, laterally convex, and increases in dorsoventral height posteriorly. Several anteroposteriorly elongated foramina are situated in the anteriormost portion of the element. Posterior to them is the *fossa premaxillaris* which extends to the posterior end of the premaxilla, as in *Palvennia hoybergeti* and *Ophthalmosaurus icenicus* (Delsett et al. 2018; Moon & Kirton 2016). In contrast, *Sveltonectes insolitus* bears a continuous groove (Fischer et al. 2011). The specimen does not seem to possess a *processus supranarialis*.

Maxilla

In lateral view, the maxilla extends anterior to the anteriormost border of the naris, and possesses a *processus narialis*. The maxilla is exposed for 40% of the total length of the premaxilla and maxilla, similar to the exposure in *Undorosaurus? kristiansenae* (38%) and *Janusaurus lundi*, and in contrast to *Aegirosaurus leptospondylus* and *Sveltonectes insolitus*, which have small maxillae relative to the other elements (Bardet & Fernández 2000; Druckenmiller et al. 2012; Fischer et al. 2011; Roberts et al. 2014). The maxilla is dorsoventrally taller than in *Undorosaurus? kristiansenae* (Druckenmiller et al. 2012). In the posterior portion, the maxilla appears toothless.

Postorbital

The postorbital is only partly preserved. Its ventral portion is anteroposteriorly widest, as in *Aegirosaurus leptospondylus* (Bardet & Fernández 2000) (SNSB-BSPG 1954 I 608, pers. observ. LLD), *Ophthalmosaurus icenicus,* and *Platypterygius australis,* in contrast to *Palvennia hoybergeti* (Delsett et al. 2018; Kear 2005; Moon & Kirton 2016).

238 **Jugal**

239 Anteriorly, the jugal only slightly exceeds the orbital margin, as is also the case for *Aegirosaurus*
240 *leptospondylus* (Bardet & Fernández 2000) and *Ophthalmosaurus icenicus* (Moon & Kirton
241 2016). Its anterior portion is of similar height throughout, as in *Athabascasaurus bitumineus*, but
242 is not as slender as in *Leninia stellans* (Druckenmiller & Maxwell 2010; Fischer et al. 2013). The
243 anterior portion of the jugal is more strongly curved than the jugal of *Undorosaurus?*
244 *kristiansenae* and *Leninia stellans*, in which it is nearly straight (Druckenmiller et al. 2012;
245 Fischer et al. 2013). The curvature of the element is more similar to *Palvennia hoybergeti*, but
246 with a shorter anterior reach (Delsett et al. 2018).
247
248 **Angular**
249 The angular is extensively exposed laterally as in *Aegirosaurus leptospondylus* and most other
250 ophthalmosaurids (Fernández & Campos 2015), in contrast to the short anterior reach in
251 *Palvennia hoybergeti* (Delsett et al. 2018). The element reaches approximately as far anteriorly
252 as the surangular, which is slightly anterior to the posterior portion of the premaxilla. The
253 angular increases in dorsoventral height in the posteriormost portion, ventral to the orbit.
254
255 **Dentary**
256 As preserved, the specimen has an underbite. If the underbite is a taphonomical artefact, it would
257 require that the lower jaw has been pushed anteriorly, as the upper jaw is not broken. This does
258 not appear likely. A real underbite is unusual among ophthalmosaurids, but is present in one
259 *Aegirosaurus leptospondylus* specimen (SNSB-BSPG 1954 I 608, pers. observ. LLD). The
260 dentary increases only slightly in dorsoventral height posteriorly, resulting in a relatively slender

element, which is more similar to *Aegirosaurus leptospondylus* than to *Palvennia hoybergeti* and *Ophthalmosaurus icenicus* (Bardet & Fernández 2000; Delsett et al. 2018; Moon & Kirton 2016).

Splenial

The right splenial is visible ventral to the surangular and angular. It is slender, and increases in thickness posteriorly. Its ventral margin is rounded, as in *Platypterygius australis* and *Palvennia hoybergeti* (Delsett et al. 2018; Kear 2005).

Dentition

On the right side, 18 teeth are preserved in the maxilla, 17 in the premaxilla and approximately 20 in the dentary, which means that the specimen has more maxillary teeth than reported for *Aegirosaurus leptospondylus* (Bardet & Fernández 2000). The teeth sit closely together in a groove that does not seem to be partitioned into alveoli. The teeth are small, straight, and gracile, more similar to *Keilhauia nui* and *Aegirosaurus leptospondylus* (Bardet & Fernández 2000; Delsett et al. 2017) (SNSB-BSPG 1954 I 608, pers. observ. LLD) than to *Ophthalmosaurus, Undorosaurus?* and *Brachypterygius extremus* (Druckenmiller et al. 2012; Kirton 1983; Moon & Kirton 2016). The margin of the enamel is straight, and the enamel does not have deep ridges.

Pectoral girdle

Three incomplete, slender elements are interpreted as the remains of one or two clavicles, and possibly the interclavicle (Fig. 2). A larger, flat element is interpreted as the coracoid, but information on notches and facets are unavailable.

284

285 **Humerus**

286 Two partial humeri (Fig. 2) with associated distal elements are preserved. The right humerus is
287 broken and only visible in cross-section. Six forelimb elements with unknown identity are
288 preserved on top of, and in immediate proximity to the humerus, and eleven elements from the
289 left forelimb are preserved partly disarticulated close to the left humerus. All elements are
290 rounded in dorsal or ventral view. Based on their size and position, it is assumed that the
291 elements originate from the proximal portion of the limb. If this is correct, it means that they
292 differ from *Aegirosaurus leptospondylus* (Bardet & Fernández 2000)(SNSB-BSPG 1954 I 608,
293 pers. observ. LLD), where the distal elements on the forelimb are almost rectangular, except for
294 the distalmost third of the limb. Rectangular forelimb elements are also found in *Platypterygius*
295 *australis, Platypterygius hercynicus, Undorosaurus? kristiansenae* and *Sveltonectes insolitus*,
296 whereas *Ophthalmosaurus icenicus* and *Palvennia hoybergeti* possess oval and circular elements
297 (Delsett et al. 2018; Druckenmiller et al. 2012; Fischer et al. 2011; Kolb & Sander 2009; Moon
298 & Kirton 2016; Zammit et al. 2010).

299

300 **Vertebral column**

301 The majority of the vertebral column is covered in fossilized soft tissue, and the centra are
302 flattened and partly decomposed (Figs. 2, 6b, e). The best preserved are the posterior dorsal and
303 the caudal vertebrae. In JME-SOS-08369, the vertebrae are larger anterior to the tail bend than
304 posterior to it. A complete series of postflexural vertebrae is preserved, with approximately 70
305 vertebrae. The number of postflexural centra and their shape is similar to the isolated tail JME-

SOS2183 described below. Two neural arches are interpreted as those of the atlas-axis and cervical vertebra 3.

The ribs are preserved articulated (Fig. 2). Most ribs do not preserve the proximal portion, but where available, they are bicipital. They possess longitudinal grooves along the entire length, giving a figure eight cross section, as is found in the majority of ophthalmosaurids, but different from *Acamptonectes densus, Mollesaurus periallus,* and three specimens from Spitsbergen (Delsett et al. 2017; Delsett et al. 2019; Fernández 1999; Fischer et al. 2012).

The abdomen (Fig. 6c, d) preserves the remains of an almost complete set of gastralia close to their position in life, probably from the left side, directed slightly posteriorly. Gastralia from the right side are situated on top of the ribs, perpendicular to the direction of the ribs. Their anteroposterior width is less than 5 mm, which is less than half the width of the ribs, and the thickness is uniform throughout. Gastralia in ophthalmosaurids are described in *Ophthalmosaurus icenicus* and specimens from the Slottsmøya Member of Spitsbergen (Delsett et al. 2018; Delsett et al. 2017; Moon & Kirton 2016; Roberts et al. 2014). In all of these, the gastralia are circular to subcircular in cross-section and with a smaller diameter compared to the thoracic ribs, as in the specimen described here. The preservation of a nearly complete gastral basket in JME-SOS-08369 is unique among ophthalmosaurids. Even for the otherwise well-known *Ophthalmosaurus icenicus*, a complete set of gastralia cannot be reconstructed, and their relationship to the dorsal rib cage is unknown (Moon & Kirton 2016).

Pelvic girdle

Two ilia (Fig. 2) are preserved, and a few elements that might originate from the hindlimbs are scattered nearby. The ilium is approximately 40 mm in dorsoventral height, slender and straight. *Aegirosaurus leptospondylus* and *Ophthalmosaurus icenicus* resemble this specimen in having ilia with a similar anteroposterior width overall, but their ilia are more curved (Bardet & Fernández 2000; Moon & Kirton 2016). In contrast, the ilia of *Keilhauia nui*, *Athabascasaurus bitumineus,* and *Undorosaurus? kristiansenae* all have one anteroposteriorly expanded end (Delsett et al. 2017).

Ichthyosauria de Blainville, 1835

Referred specimen JME-SOS2183 (Fig. 3). The specimen is housed in the Jura-Museum Eichstätt, Eichstätt, Germany.

Locality The Eichstätt-Blumenberg area. The exact location is not known.

Age early Tithonian, Late Jurassic.

Taxonomic assignment

JME-SOS2183 (Fig. 3) only consists of a tail. There are no diagnostic characters in the tail for Ophthalmosauridae, and the specimen is thus referred to Ichthyosauria indet.. Based on its strong similarity to other, more complete specimens from Solnhofen, it most likely belongs in Ophthalmosauridae.

Description and comparison JME-SOS2183

The specimen preserves the peduncle, and the entire caudal fin posterior to it (Fig. 3). As the nearly complete specimen JME-SOS-08369, it preserves a soft tissue outline, only described previously in ophthalmosaurids in the neotype of *Aegirosaurus leptospondylus* and in a specimen lost in WWII ("Tail Munich State Museum" TMSM), both from Solnhofen (Bardet & Fernández 2000; Bauer 1898; Merriam 1908). The soft tissue outline of the caudal fin is better developed in JME-SOS2183 than in JME-SOS-08369 and demonstrates that the tail had the classical lunate shape in lateral view as in other Jurassic ichthyosaurs, such as *Stenopterygius* specimens from of Holzmaden. As in the nearly complete specimen JME-SOS-08369, the peduncle of JME-SOS2183 is dorsoventrally narrow and widens dorsally and ventrally into the caudal fin. The dorsal lobe tip is dorsoventrally shorter and anteroposteriorly longer than the ventral portion. The tip of the dorsal lobe is also angled more posteriorly compared to the tip of its ventral lobe. This might however be a taphonomic artefact of preservation and/ or preparation, as a crack extends through the matrix and fossil at this point.

Vertebral column

Six caudal vertebrae are preserved articulated anterior to the tail bend and are significantly larger (heights 14-18 mm and length 7-8 mm) than those posterior to the bend. The posterior caudal vertebrae are amphicoelous, and equally anteroposteriorly long dorsally and ventrally. The vertebrae forming the tail bend are not preserved.

Approximately 70 small postflexural vertebrae are preserved in articulation. This is similar to the nearly complete specimen JME-SOS-08369 and to the TMSM (Bardet & Fernández 2000; Bauer 1898; Merriam 1908). The neotype of *Aegirosaurus leptospondylus* preserves the entire tail, with

61 postflexural centra (Bardet & Fernández 2000). The dorsoventral height and anteroposterior length of all the postflexural vertebrae in JME-SOS2183 are similar, giving a quadratic outline in lateral view (height = 5 mm, length = 5 mm). Consequently, they are anteroposteriorly longer than those anterior to the tail bend, as in the TMSM specimen (Merriam 1908). The exception are the miniature vertebrae at the very end of the tail. This is similar to some specimens of *Ophthalmosaurus icenicus* (Moon & Kirton 2016), but see (Buchholtz 2001). Height is also slightly larger than length in the postflexural vertebrae of *Acamptonectes densus* (Fischer et al. 2012: SNHM 1284-R, fig. 8), *Sveltonectes insolitus* (Fischer et al. 2011), and *Arthropterygius* (Maxwell 2010).

Results – characterization of soft tissue

Several different types of soft tissue are preserved in the nearly complete specimen JME-SOS-08369, based on observation in UV, regular and low angle light (Figs. 2, 4, 6, 7). Here, we discuss two types (type I and II). In addition, the abdomen and pelvic girdle regions especially preserve additional types of soft tissue that should be considered for analysis. No scale impressions are observed on any of the specimens. A rectangular lump of fossilized soft tissue in the approximate anteroposterior midpoint of the dorsal outline might represent the remnants of a folded dorsal fin (Fig. 6b). Stomach content was not observed.

Type I is a thick, outer phosphatic layer, preserved with an off-white color, with yellowish fluorescence (Fig. 6a, b, e, f). It can be observed along the dorsal outline of the specimen starting from the posterior end of the skull; posterior to the pelvic girdle, and in the ventral portion of the tail. During preparation, an additional soft tissue type layered with Type I was observed

(Radecker 2014), but this layer is now preserved only in a few smaller patches. **Type II** is the most common type of preservation of soft tissue in JME-SOS-08369 (Fig 2, 6a, d, e, f). It is an amorphous and light yellow substance infilling large parts of the specimen, covering many of the skeletal elements. Both type I and type II soft tissue are preserved as incrustation pseudomorphs (epimorphs), with no sign of subcellular preservation.

The remnants of soft tissue in the isolated tail JME-SOS2183 is preserved around the entire specimen, and was likely enhanced by the addition of some sort of stabilizer/lacquer many years ago (Andreas Radecker, pers. comm.). Type I soft tissue preservation as seen on the leading edge of the caudal fin differs from that on the posterior margin, and seems more robust and probably had a stiffening function. On the dorsal leading edge, this tissue is segmented.

XRD analyses of material in two samples (JME-SOS-08369-B1 and B2, Fig. 4) that appear off-white in regular light and fluorescent light yellow in UV light, match apatite and is likely referable to type I soft tissue. The same color in UV light is present in the isolated tail JME-SOS2183 in the leading edge of the dorsal lobe of the tail, corresponding to the position of the analyzed samples from JME-SOS-08369, probably representing the same type of mineralized soft tissue. The light beige matrix present on all analyzed samples (JME-SOS-08369-B1, B2 and B3) fits calcite, as expected for limestone.

XRD cannot distinguish between the various members of the apatite group, and chemical data is required to confirm the identification. The semi-quantitative analyses (EDS) (Fig. 7) confirm that

421 the matrix is calcite containing minor amounts of Mg and a silicate mineral, but no phosphates.
422 The material identified via XRD as apatite contains P, Ca, O and F as the main constituents, with
423 minor Na and S, and is consistent with fluorapatite. Apart from Ca and O these elements were
424 only observed in the off-white -colored material. The analyzed samples also have some black
425 material, which is found to be iron oxide with minor Mn. The humeri were covered with a late
426 encrustation of iron hydroxide when excavated (Radecker 2014).
427
428 To determine whether the phosphorous could result from an internal source, we calculated
429 whether the soft tissues in a similar-sized cetacean could produce sufficient amount of
430 phosphorous for the observed amount of phosphatized soft tissue in the nearly complete
431 specimen JME-SOS-08369 (Supplementary material 1). The calculations on the amount of
432 phosphorous in the soft tissue (blubber, skin, muscles) for an ichthyosaur this size, yield a total
433 of 32 g phosphorus. The density of fluorapatite is 3.2 g/cm^3, which means the decomposition of
434 the specimen could create 54 cm^3 pure fluorapatite. Based on its outline (Fig. 2), the area of the
435 specimen is 6560 cm^2, which means that if the apatite formed a single solid crystal under the
436 fossil it could be 0.8 mm thick. The apatite is not a solid crystal, but will form on the particles
437 within the sediment and pores around the specimen. Consequently, the zone containing apatite
438 could be thicker than 0.8 mm just from phosphorus derived from the soft tissue, even without
439 taking into account the phosphate derived from the later decomposition of the skeleton. It should
440 be highlighted that by using ideal fluorapatite in our calculation, the amount of apatite that can
441 be formed is a minimum value. For example, the incorporation of carbonate groups for
442 phosphate groups in the apatite structure, would result in more apatite formed, as the content of P
443 in carbonate apatite is smaller than in fluorapatite. That is, the more carbonate that substitutes for

444 phosphorous in the apatite, the more apatite can be formed from the same amount of P. The
445 incorporation of carbonate for phosphorous in apatite also leads to a reduction in density, which
446 means that for the same weight of apatite formed, carbonate-rich apatite will have a larger
447 volume than the same weight of fluorapatite. Consequently, with carbonates substituting for
448 some P in the apatite structure, two effects will increase the volume of apatite that forms.
449
450

451 Discussion

452 Soft tissue

453 Type I soft tissue, found along the margins of the body of the nearly complete specimen JME-
454 SOS-08369 and surrounding the tail in JME-SOS2183, is interpreted as smooth epidermis and
455 dermis, possibly including connective tissue in the tail. Previous analysis found that the dermis
456 and epidermis were multi-layered, as in modern tetrapods (Lindgren et al. 2018), which fits with
457 the observation during preparation of at least two layers of soft tissue (Radecker 2014).
458

459 In the dorsal portion of the tail of the SM neotype of *Aegirosaurus leptospondylus*, Bardet and
460 Fernández (2000, p. 508) observed minute, rounded 'scale structures' interpreted as scales
461 covering the skin. This contrasts with the specimens described here, which are in line with other
462 recent studies, where ichthyosaur skin is interpreted to be smooth (Lindgren et al. 2018).
463

464 Type II soft tissue resembles mostly the light yellow, amorphous substance also observed by
465 Lindgren et al. (2018) in a *Stenopterygius* specimen (MH432), and interpreted by them as
466 adipocere from decomposed blubber. Under conditions with little or no oxygen, microorganisms

467 produce polyhydroxy fatty acids from fatty tissues from a surplus of organic compounds,
468 commonly known as adipocere (Schoenen & Schoenen 2013).
469
470 The EDS and XRD analyses (Fig. 7) show that the soft tissue in the tail of the nearly complete
471 specimen JME-SOS-08369 is phosphatized, likely by francolite, as is common in vertebrate soft
472 tissue from Solnhofen (Barthel et al. 1990). As most of the fossilized soft tissue in vertebrates
473 from the Solnhofen area preserve subcellular details, Wilby (1993) and Wilby et al. (1995)
474 suggested a supersaturated (probably sedimentary) source of phosphorus, because of depleted
475 levels of sedimentary phosphate adjacent to the fossils (Briggs 2003; Briggs & Wilby 1996).
476 This is in contrast to the phosphatization in the Santana Formation (Brazil), which is interpreted
477 as authigenic mineralization due to decomposition of remains containing phosphate (Briggs
478 2003; Briggs et al. 1993; Martill 1988). JME-SOS-08369 shows no sign of subcellular
479 preservation. The phosphate mineralization is instead observed as incrustation pseudomorphs
480 (epimorphs), resulting from a process by which the soft tissue is coated by apatite, and the
481 encased tissue decomposes. The encasing phosphate remains intact as a thin sheet and retains the
482 outer shape of the original tissue.
483

484 **Source of the phosphorous**

485 The calculations showed that these tissues could provide sufficient P for the formation of a 0.8
486 mm thick layer of fluorapatite, i.e. sufficient for the observed preservation of mineralized
487 epimorphs of soft tissue. The other main component of apatite is Ca, found in abundance
488 throughout the host rock (Fig. 7). The skeleton is a possible phosphorous source, and the visible
489 decomposition of vertebrae and ribs may have contributed to the apatite formation. However, the

apatite layer is not concentrated around the skeletal elements, but rather through the entire area covered by the specimen.

We conclude that an external phosphorous source is not necessary for this type of preservation to occur. In addition to muscles, we argue that the ichthyosaur possessed blubber, based on our observations of Type II soft tissue, in accordance with previous work (Lindgren et al. 2018). Thus, the phosphorus in the mineralized soft tissue is most likely derived from the most local source, the decaying organic matter of the ichthyosaur itself. A local source of phosphorus rather than external is further supported by the detailed investigation of the specimen and the element mapping (Fig. 7), which show phosphorus only in the area where the fossil is preserved. If the phosphorus source was external, it seems unlikely that apatite only formed where the fossil is preserved. However, as analyses of modern whale-falls have shown that there is an exchange of chemical components between decaying carcasses and the surrounding sediments, an external phosphorous source cannot be completely excluded.

Phosphatization of tissues normally occur within the sediment (Martill 1993). In Solnhofen, fully articulated skeletons with mineralized soft-tissue preservation are hypothesized to have been buried within a few weeks (Kemp & Trueman 2003). The observed preservation of the ichthyosaur is possible because of a short post-mortem floatation with rapid burial and/or overgrowth by microbial films. Rapid burial is due to sediments transported into the basin during storm events. Together with a quick re-establishment of the pycnocline after storm events with hypersaline, oxygen-poor to anoxic bottom waters these conditions make the exceptional preservation possible (Pan et al. 2019).

Phosphatization of soft tissue in a carbonate-dominated environment, as in the Solnhofen area, has been hypothesized to be dependent on an anoxic environment with low pH (Briggs 2003; Briggs & Wilby 1996). In larger vertebrate carcasses, another possible scenario is that the skin creates a local closed system and an elevated concentration of phosphorous during decay. This creates a local fall in pH, shifting the equilibrium away from favouring precipitation of carbonate, to francolite (Briggs 2003; Briggs & Wilby 1996; Gueriau et al. 2020).

The source of fluorine in francolite can be explained by the bioapatite presence in the animal, as fluoride incorporation is prevalent although typically low ow with higher concentration close to veins and tissue (Li & Pasteris 2014). Francolite is known to form by precipitation from anoxic porewater, replacement of carbonate, bacterial processes, post-mortem precipitation of francolite in phosphorus-rich bacterial cells; and possibly by precipitation from the water-column at the sediment water interface (McArthur 1985).

The minor amounts of Na and S in fluorapatite can be explained by the coupled substitution $Ca^{2+} + P^{5+} \rightarrow Na^{+} + S^{6+}$, typical for apatite-group minerals, where Na and S originate from the sea water. In addition, iron was observed through SEM-EDS as well as during preparation, where iron oxide covered some of the elements (Radecker 2014). This fits well with iron-rich bands observed in SEM-EDS, which are not present in the areas with apatite. The iron oxides and hydroxides are also most likely late weathering products, after the deposits became subaerial in the Cretaceous-Paleogene.

Conclusion

Two ichthyosaur specimens from the Solnhofen Archipelago represent rare cases of soft tissue preservation in ophthalmosaurids, including skin, potential blubber and additional tissue types. The phosphate mineralization is observed as incrustation pseudomorphs (epimorphs) on the soft tissue. SEM and XRD analyses revealed the presence of fluorapatite within the boundary of the fossil. The phosphorus likely originated from the tissues of the ichthyosaur, and does not require an external source. This finding is of interest for understanding the taphonomical pathways of large Solnhofen vertebrates. For future work, microscopical and geochemical analysis of different parts of the specimens have the potential to reveal more information Hopefully, additional work on these specimens can be done at a later stage, with targeted analyses of all different soft tissue types.

The specimens also hold the potential for future investigations into locomotion in derived ichthyosaurs, as the entire body, including two tails, preserve soft tissue outline in combination with probable blubber and some of the most complete ophthalmosaurid tail skeletons described.

Institutional abbreviations

JME, Jura-Museum Eichstätt, Eichstätt, Germany, specimens belong to the collection of the Bishops Seminar Eichstätt;

SNSB-BSPG, Bayerische Staatssammlung für Paläontologie und Geologie, Munich, Germany.

Acknowledgements

Specimen JME-SOS-08369 belongs to the collection of the Bishops Seminar Eichstätt, who kindly permitted access to the specimen. Access was granted by the Jura-Museum Eichstätt. We thank A. Radecker warmly for preparing JME-SOS-08369 and for being an important source of knowledge as well as practical support. We also thank M. Ebert for his hospitality during LLD and JHH's visit to Eichstätt and the Jura-Museum, and O. Rauhut for his help during LLD's visit to the collection in Munich. We thank C. Ifrim, H. A. Nakrem, D. Larsen, K. L. Voje, G. Gundersen, and N. Castro for administrative and lab support. We thank editors and reviewers for comments that greatly improved the manuscript.

References

Bardet N, and Fernández MS. 2000. A new ichthyosaur from the Upper Jurassic lithographic limestones of Bavaria. *Journal of Paleontology* 74:503-511.

Barthel KW. 1970. On the deposition of the Solnhofen lithographic limestone (Lower Tithonian, Bavaria, Germany). *Neues Jahrbuch Für Geologie Und Paläontologie - Abhandlungen* 135:1–18.

Barthel KW, Swinburne NHM, and Morris SC. 1990. *Solnhofen. A Study in Mesozoic Palaeontology.* Cambridge: Cambridge University Press.

Bauer F. 1898. Die Ichthyosaurier des oberen weissen Jura. *Palaeontographica* 44:283–328.

Baur G. 1887. On the morphology and origin of the Ichthyopterygia. *American Naturalist* 21:837-840.

Briggs DEG. 2003. The role of decay and mineralization in the preservation of soft-bodied fossils. *Annual Review of Earth and Planetary Sciences* 31:275-301. 10.1146/annurev.earth.31.100901.144746

Briggs DEG, Kear AJ, Martill DM, and Wilby PR. 1993. Phosphatization of soft-tissue in experiments and fossils. *Journal of the Geological Society* 150:1035-1038.

Briggs DEG, and Wilby PR. 1996. The role of the calcium carbonate-calcium phosphate switch in the mineralization of soft-bodied fossils. *Journal of the Geological Society* 153:665-668. 10.1144/gsjgs.153.5.0665

Buchholtz EA. 2001. Swimming styles in Jurassic ichthyosaurs. *Journal of Vertebrate Paleontology* 21:61–73. 10.1671/0272-4634(2001)021[0061:SSIJI]2.0.CO;2

Böttcher R. 1990. Neue Erkenntnisse über die Fortpflanzungsbiologie der Ichthyosaurier (Reptilia). *Stuttgarter Beiträge zur Naturkunde Serie B (Geologie und Paläontologie)* 164:1–51.

Cozzi B, Huggenberger S, and Oelschläger H. 2017. *Anatomy of Dolphins. Insights into Body Structure and Function*. London: Academic Press.

de Blainville MHD. 1835. Description de quelques espèces de reptiles de la Californie, précédée de l'analyse d'un systéme général d'erpétologie et d'amphibiologie. *Nouvelles Annales du Muséum d'Histoire Naturelle* 4:233–296.

Delsett LL, Druckenmiller PS, Roberts AJ, and Hurum JH. 2018. A new specimen of *Palvennia hoybergeti*: implications for cranial and pectoral girdle anatomy in ophthalmosaurid ichthyosaurs. *PeerJ* e5776. 10.7717/peerj.5776

Delsett LL, Roberts AJ, Druckenmiller PS, and Hurum JH. 2017. A new ophthalmosaurid (Ichthyosauria) from Svalbard, Norway, and evolution of the ichthyopterygian pelvic girdle. *PLoS ONE* 12:e0169971. 10.1371/journal.pone.0169971

Delsett LL, Roberts AJ, Druckenmiller PS, and Hurum JH. 2019. Osteology and phylogeny of Late Jurassic ichthyosaurs from the Slottsmøya Member Lagerstätte (Spitsbergen, Norway). *Acta Palaeontologica Polonica* 64:717–743. 10.4202/app.00571.2018

Druckenmiller PS, Hurum JH, Knutsen EM, and Nakrem HA. 2012. Two new ophthalmosaurids (Reptilia: Ichthyosauria) from the Agardhfjellet Formation (Upper Jurassic: Volgian/Tithonian), Svalbard, Norway. *Norwegian Journal of Geology* 92:311–339.

Druckenmiller PS, and Maxwell EE. 2010. A new Lower Cretaceous (lower Albian) ichthyosaur genus from the Clearwater Formation, Alberta, Canada. *Canadian Journal of Earth Sciences* 47:1037–1053. 10.1139/e10-028

Fernández MS. 1999. A new ichthyosaur from the Los Molles Formation (early Bajocian), Neuquen Basin, Argentina. *Journal of Paleontology* 73:677–681.

Fernández MS, and Campos L. 2015. Ophthalmosaurids (Ichthyosauria: Thunnosauria): alpha taxonomy, clades and names. *Publicación Electrónica de la Asociación Paleontológica Argentina* 15:20–30. 10.5710/PEAPA.15.09.2015.96

Fischer V, Arkhangelsky MS, Uspensky GN, Stenshin IM, and Godefroit P. 2013. A new Lower Cretaceous ichthyosaur from Russia reveals skull shape conservatism within Ophthalmosaurinae. *Geological Magazine* 151:60–70. doi:10.1017/S0016756812000994

Fischer V, Bardet N, Benson RBJ, Arkhangelsky MS, and Friedman M. 2016. Extinction of fish-shaped marine reptiles associated with reduced evolutionary rates and global environmental volatility. *Nature Communications* 7:10825. 10.1038/ncomms10825

Fischer V, Maisch MW, Naish D, Kosma R, Liston J, Joger U, Krüger FJ, Pardo-Pérez JM, Tainsh J, and Appleby RM. 2012. New ophthalmosaurid ichthyosaurs from the European Lower Cretaceous demonstrate extensive ichthyosaur survival across the Jurassic–Cretaceous boundary. *PLoS ONE* 7:e29234. 10.1371/journal.pone.0029234

Fischer V, Masure E, Arkhangelsky MS, and Godefroit P. 2011. A new Barremian (Early Cretaceous) ichthyosaur from Western Russia. *Journal of Vertebrate Paleontology* 31:1010–1025. 10.1080/02724634.2011.595464

Fraas E. 1888. Über die Finne von *Ichthyosaurus*. *Jahreshefte des Vereins für vaterländische Naturkunde in Württemberg* 44:280–303.

Gueriau P, Bernard S, Farges F, Mocuta C, Dutheil DB, Adatte T, Bomou B, Godet M, Thiaudière D, Charbonnier S, and Bertrand L. 2020. Oxidative conditions can lead to exceptional preservation through phosphatization. *Geology* 48:1164–1168.

Gäb F, Ballhaus C, Stinnesbeck E, Kral AG, Janssen K, and Bierbaum G. 2020. Experimental taphonomy of fish - role of elevated pressure, salinity and pH. *Scientific Reports* 10:7839. 10.1038/s41598-020-64651-8

Haug C, Haug JT, Waloszek D, Maas A, Frattigiani R, and Liebau S. 2009. New methods to document fossils from lithographic limestones of Southern Germany and Lebanon. *Palaeontologia Electronica* 12.3.6T.

Huene Fv. 1922. *Die Ichthyosaurier des Lias und ihre Zusammenhänge*. Berlin: Verlag von Gebrüder Borntraeger.

Jaekel O. 1904. Eine neue Darstellung von *Ichthyosaurus. Zeitschrift der Deutschen Geologischen Gesellschaft* 56:26–34.

Kear BP. 2005. Cranial morphology of *Platypterygius longmani* Wade, 1990 (Reptilia: Ichthyosauria) from the Lower Cretaceous of Australia. *Zoological Journal of the Linnean Society* 145:583–622. 10.1111/j.1096-3642.2005.00199.x

Kemp RA, and Trueman CN. 2003. Rare earth elements in Solnhofen biogenic apatite: geochemical clues to the palaeoenvironment. *Sedimentary Geology* 155:109-127. 10.1016/S0037-0738(02)00163-X

Kirton AM. 1983. A review of British Upper Jurassic Ichthyosaurs Unpublished PhD thesis. Unpublished PhD thesis, University of Newcastle upon Tyne.

Knudsen AC, and Gunter ME. 2002. Sedimentary phosphorites—an example: Phosphoria Formation, Southeastern Idaho, U.S.A. *Reviews in Mineralogy and Geochemistry* 48:363-389.

Koch R, Senowbari-Daryan B, and Strauss H. 1994. The Late Jurassic "Massenkalk Fazies" of Southern Germany: Calcareous sand piles rather than organic reefs. *Facies* 31:179-208.

Kolb C, and Sander PM. 2009. Redescription of the ichthyosaur *Platypterygius hercynicus* (Kuhn 1946) from the Lower Cretaceous of Salzgitter (Lower Saxony, Germany). *Palaeontographica Abteilung A: Paläozoologie - Stratigraphie* 288:151–192.

Kölbl-Ebert M, Röper M, and Leinfelder RR. 2005. *4th International Symposium on Limestone and Plattenkalk.* Eichstätt/ Solnhofen, Germany, 26 pp.: Zitteliana.

Li Z, and Pasteris JD. 2014. Chemistry of bone mineral, based on the hypermineralized rostrum of the beaked whale *Mesoplodon densirostris. American Mineralogist* 99:645-653. doi:10.2138/am.2014.4571

Lindgren J, Sjövall P, Carney RM, Uvdal P, Gren JA, Dyke G, Schultz BP, Shawkey MD, Barnes KR, and Polcyn MJ. 2014. Skin pigmentation provides evidence of convergent melanism in extinct marine reptiles. *Nature* 506:484–488. 10.1038/nature12899

Lindgren J, Sjövall P, Thiel V, Zheng W, Ito S, Wakamatsu K, Hauff R, Kear BP, Engdahl A, Alwmark C, Eriksson ME, Jarenmark M, Sachs S, Ahlberg PE, Marone F, Kuriyama T, Gustafsson O, Malmberg P, Thomen A, Rodríguez-Meizoso I, Uvdal P, Ojika M, and Schweitzer MH. 2018. Soft-tissue evidence for homeothermy and crypsis in a Jurassic ichthyosaur. *Nature* 564:359–365. 10.1038/s41586-018-0775-x

Lydekker R. 1889. On an ichthyosaurian paddle showing the contour of the integuments. *Geological Magazine* 6:388–390.

M'Coy F. 1867. On the occurrence of Ichthyosaurus and Plesiosaurus in Australia. *Annals and magazine of natural history* 19:355–356.

Martill DM. 1987. A taphonomic and diagenetic case-study of a partially articulated ichthyosaur. *Palaeontology* 30:543–555.

Martill DM. 1988. Preservation of fish in the Cretaceous Santana Formation of Brazil. *Palaeontology* 31:1-18.

Martill DM. 1993. Soupy substrates: a medium for the exceptional preservation of ichthyosaurs of the Posidonia Shale (Lower Jurassic) of Germany. *Kaupia Darmstädter Beiträge zur Naturgeschichte* 2:77–97.

Martill DM. 1995. An ichthyosaur with preserved soft tissue from the Sinemurian of southern England. *Palaeontology* 38:897–903.

Martin J, Frey E, and Riess J. 1986. Soft tissue preservation in ichthyosaurs and a stratigraphic review of the Lower Hettangian of Barrow-upon-Soar, Leicestershire. *Transactions of the Leicester Literary & Philosophical Society* 80:58–72.

687 Maxwell EE. 2010. Generic reassignment of an ichthyosaur from the Queen Elizabeth Islands, Northwest
688 Territories, Canada. *Journal of Vertebrate Paleontology* 30:403–415.
689 10.1080/02724631003617944
690 Maxwell EE. 2012a. New metrics to differentiate species of *Stenopterygius* (Reptilia: Ichthyosauria) from
691 the Lower Jurassic of southwestern Germany. *Journal of Paleontology* 86:105–115. 10.1666/11-
692 038.1
693 Maxwell EE. 2012b. Unraveling the influences of soft-tissue flipper development on skeletal variation
694 using an extinct taxon. *Journal of experimental zoology molecular and developmental evolution*
695 318B:545–554. 10.1002/jez.b.22459
696 Maxwell EE, and Caldwell MW. 2006. A new genus of ichthyosaur from the Lower Cretaceous of
697 Western Canada. *Palaeontology* 49:1043–1052. 10.1111/j.1475-4983.2006.00589.x
698 McArthur JM. 1985. Francolite geochemistry—compositional controls during formation, diagenesis,
699 metamorphism and weathering. *Geochimica et Cosmochimica Acta* 49:23-35. 10.1016/0016-
700 7037(85)90188-7
701 Merriam JC. 1908. Triassic Ichthyosauria, with special reference to the American forms. *Memoirs of the*
702 *University of California* 1:1–193.
703 Meyer Hv. 1863. *Ichthyosaurus leptospondylus* Wag.? aus dem lithographischen Schiefer von Eichstätt.
704 *Palaeontographica* 11:222-225.
705 Moon BC. 2017. A new phylogeny of ichthyosaurs (Reptilia: Diapsida). *Journal of Systematic*
706 *Palaeontology* 17:129–155. 10.1080/14772019.2017.1394922
707 Moon BC, and Kirton AM. 2016. Ichthyosaurs of the British Middle and Upper Jurassic. Part 1
708 *Ophthalmosaurus. Monograph of the Palaeontographical Society* 170:1–84.
709 Motani R. 1999. Phylogeny of the Ichthyopterygia. *Journal of Vertebrate Paleontology* 19:473-496.
710 Munnecke A, Westphal H, and Kölbl-Ebert M. 2008. Diagenesis of plattenkalk: examples from the
711 Solnhofen area (Upper Jurassic, southern Germany). *Sedimentology* 55:1931–1946.
712 Owen R. 1841. A description of some of the soft parts, with the integument, of the hind-fin of the
713 *Ichthyosaurus*, indicating the shape of the fin when recent. *Transactions of the Geological*
714 *Society of London* 6:199–201. 10.1144/transgslb.6.1.199
715 Pan Y, and Fleet ME. 2002. Compositions of the apatite-group minerals: substitution mechanisms and
716 controlling factors. *Reviews in Mineralogy and Geochemistry* 48:13-49.
717 Pan Y, Fürsich FT, Chellouche P, and Hu L. 2019. Taphonomy of fish concentrations from the Upper
718 Jurassic Solnhofen Plattenkalk of Southern Germany. *Neues Jahrbuch Für Geologie Und*
719 *Paläontologie - Abhandlungen* 292:73-92.
720 Pasero M, Kampf AR, Ferraris C, Pekov IV, Rakovan J, and White TJ. 2010. Nomenclature of the apatite
721 supergroup minerals. *European Journal of Mineralogy* 22:163-179. 10.1127/0935-
722 1221/2010/0022-2022
723 Radecker A. 2014. Präparation eines Ichthyosauriers aus dem Blumenberg. *Archaeopteryx* 32:57–61.
724 Rauhut OWM, Foth C, and Tischlinger H. 2018. The oldest *Archaeopteryx* (Theropoda: Avialiae): a new
725 specimen from the Kimmeridgian/Tithonian boundary of Schamhaupten, Bavaria. *PeerJ* 6:e4191.
726 10.7717/peerj.4191
727 Renesto S, Dal Sasso C, Fogliazza F, and Ragni C. 2020. New findings reveal that the Middle Triassic
728 ichthyosaur *Mixosaurus cornalianus* is the oldest amniote with a dorsal fin. *Acta Palaeontologica*
729 *Polonica* 65:511–522.
730 Roberts AJ, Druckenmiller PS, Sætre G-P, and Hurum JH. 2014. A new Upper Jurassic ophthalmosaurid
731 ichthyosaur from the Slottsmøya Member, Agardhfjellet Formation of Central Spitsbergen. *PLoS*
732 *ONE* 9:e103152. 10.1371/journal.pone.0103152

733 Schoenen D, and Schoenen H. 2013. Adipocere formation—the result of insufficient microbial
734 degradation. *Forensic Science International* 226:301.e301-301.e306.
735 10.1016/j.forsciint.2013.01.023
736 Seeley HG. 1874. On the pectoral arch and fore limb of *Ophthalmosaurus*, a new ichthyosaurian genus
737 from the Oxford Clay. *Quarterly Journal of the Geological Society* 30:696–707.
738 10.1144/gsl.jgs.1874.030.01-04.64
739 Wagner A. 1853. Die Characteristic einer neuen Art von *Ichthyosaurus* aus den lithographischen
740 Schiefern und eines Zahnes von *Polyptychodon* aus dem Gründsandsteine von Kelheim. *Bulletin*
741 *der königlische Akademie der Wissenschaft, Gelehrte Anzeigen* 3:25–35.
742 Whitear M. 1956. On the colour of an ichthyosaur. *Annals and magazine of natural history* 9:742–744.
743 10.1080/00222935608655889
744 Wilby PR. 1993. The role of organic matrices in post-mortem phosphatization of soft tissues. *Kaupia*
745 *Darmstädter Beiträge zur Naturgeschichte* 2:99-113.
746 Wilby PR, and Briggs DEG. 1997. Taxonomic trends in the resolution of detail preserved in fossil
747 phosphatized soft tissues. *Geobios* 30:493–502. 10.1016/S0016-6995(97)80056-3
748 Wilby PR, Briggs DEG, and Viohl G. 1995. Controls on the phosphatization of soft tissues in plattenkalks.
749 2nd International Symposium Lithographic Limestones. Cuenca, Spain: Autonoma Madrid.
750 Zammit M, Norris RM, and Kear BP. 2010. The Australian Cretaceous ichthyosaur *Platypterygius*
751 *australis*: a description and review of postcranial remains. *Journal of Vertebrate Paleontology*
752 30:1726–1735. 10.1080/02724634.2010.521930

753

Figure 1

Map showing the Solnhofen area in Germany, and the Eichstätt-Blumenberg visitor quarry (latitude 48.9˚N, longitude 11˚ E) where the ichthyosaur specimens were found. Modified from Barthel et al. 1990.

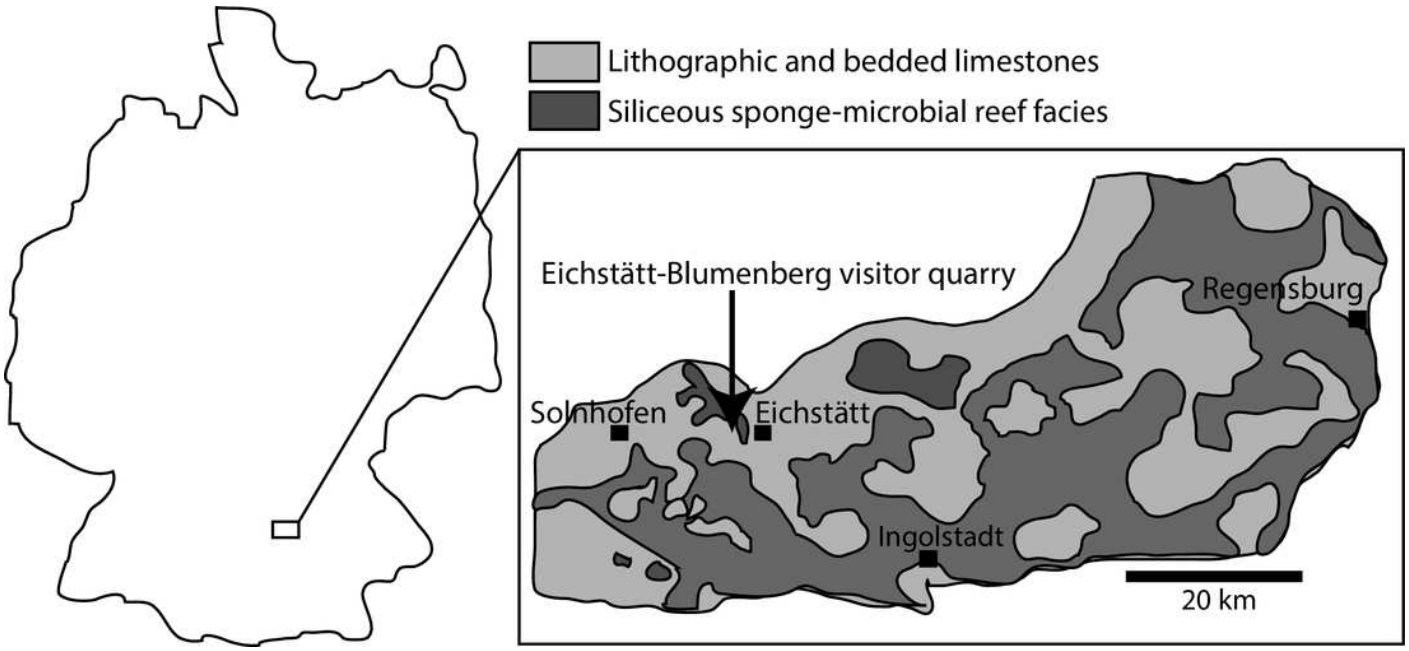

Figure 2

Late Jurassic *Aegirosaurus* sp. (JME-SOS-08369) from Eichstätt-Blumenberg, Germany.

(A) in normal light. **(B)** composite picture in UV light indicating position of pictures in figure 6. **(C)** interpretative drawing. L = left, R = right. Type I and II soft tissue marked. Scale bar = 20 cm.

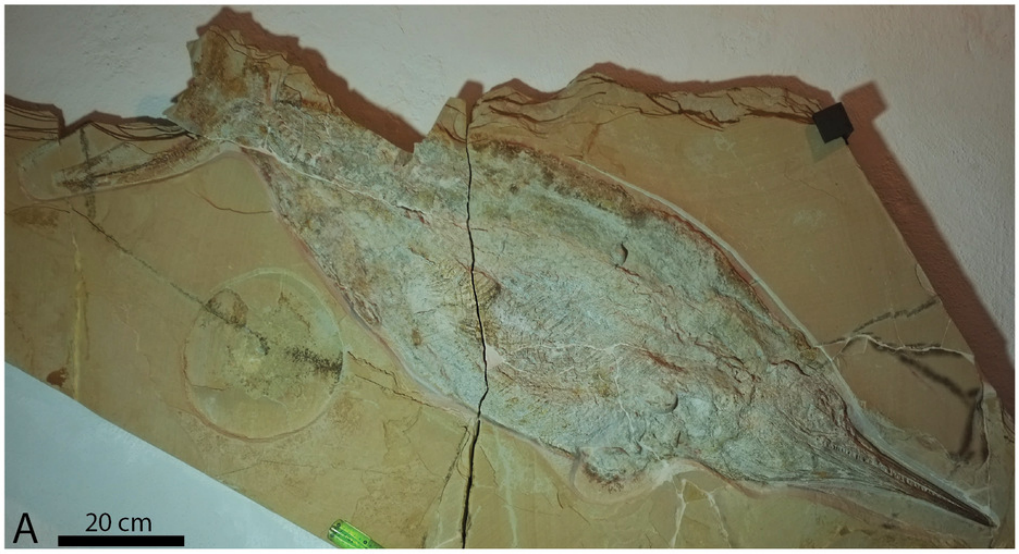
A
20 cm

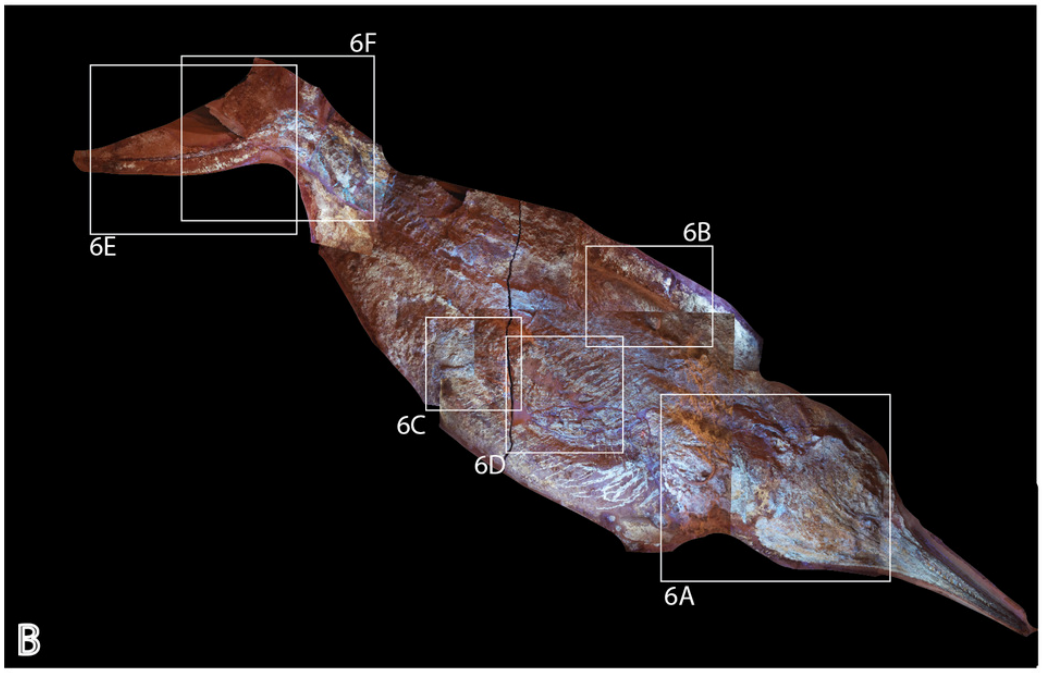
6F
6E
6B
6C
6D
6A
B

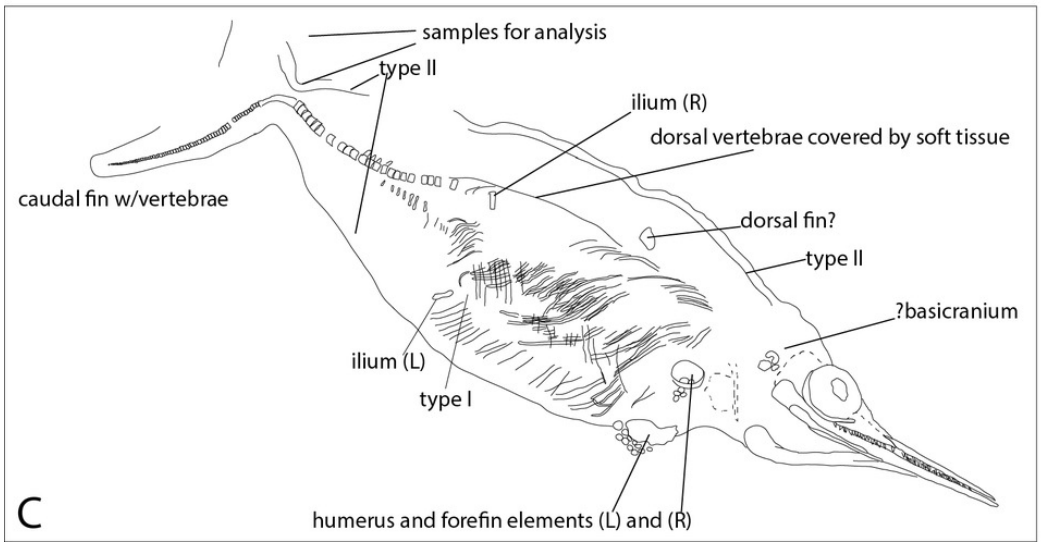
samples for analysis
type II
ilium (R)
dorsal vertebrae covered by soft tissue
caudal fin w/vertebrae
dorsal fin?
type II
?basicranium
ilium (L)
type I
C
humerus and forefin elements (L) and (R)

Figure 3

Late Jurassic ichthyosaur tail (JME-SOS2183) from Eichstätt-Blumenberg, Germany.

(A) Regular light. **(B)** Ultraviolet light. **(C)** Interpretative drawing. Scale bar = 10 cm.

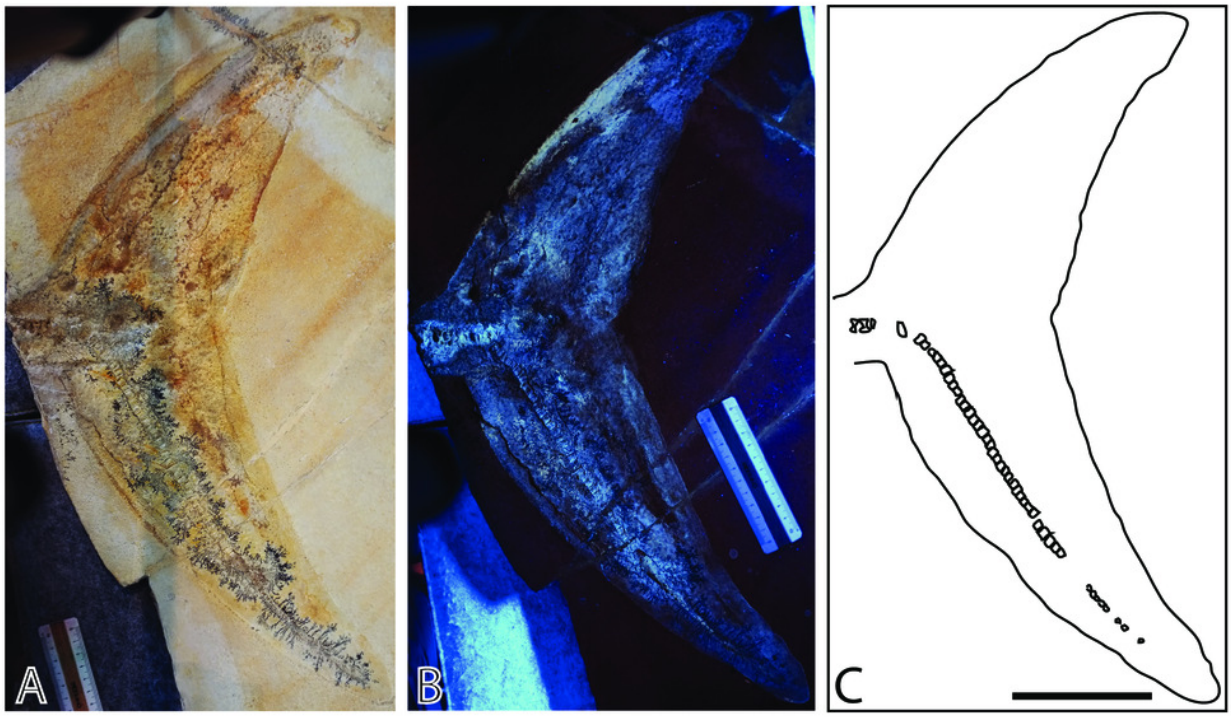

Figure 4

Samples analyzed from Late Jurassic *Aegirosaurus* sp. (JME-SOS-08369), for possible soft tissue.

Sample JME-SOS-08369-B1 in **(A)** normal light and **(B)**, UV light. Sample JME-SOS-08369-B2 in **(C)**, normal light and **(D)**, UV light. Sample JME-SOS-08369-B3 in **(E)**, normal light and **(F)**, UV light. Arrows in B and D on areas where soft tissue epimorphs (apatite) were preserved.

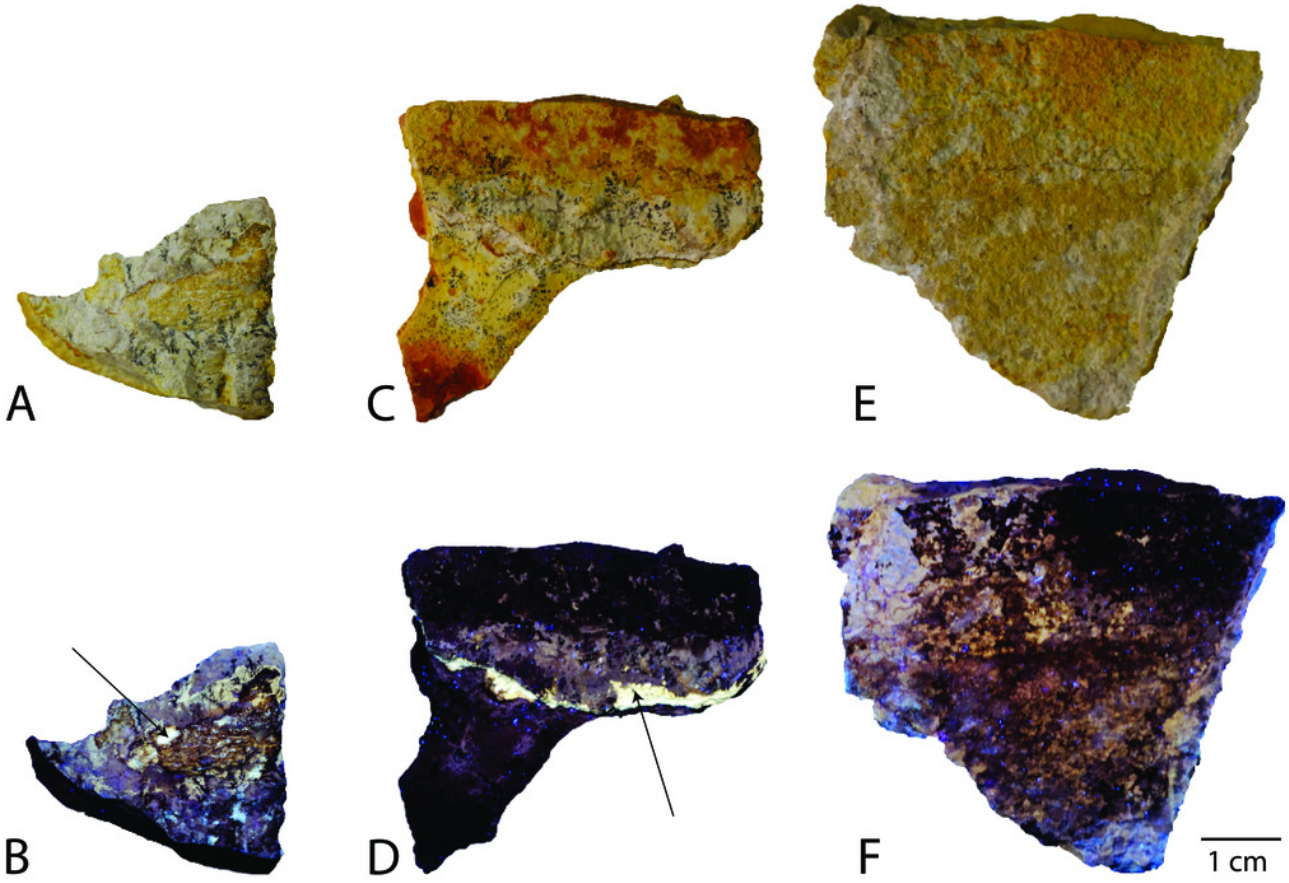

Figure 5

Interpretative drawing of the skull of Late Jurassic *Aegirosaurus* sp. (JME-SOS-08369) from Eichstätt-Blumenberg, Germany.

Abbreviations: an = angular, ar = articular, dt = dentary, j = jugal, mx = maxilla, pmax = premaxilla, po = postorbital, sa = surangular, sp = splenial, st = supratemporal. Scale bar = 5 cm.

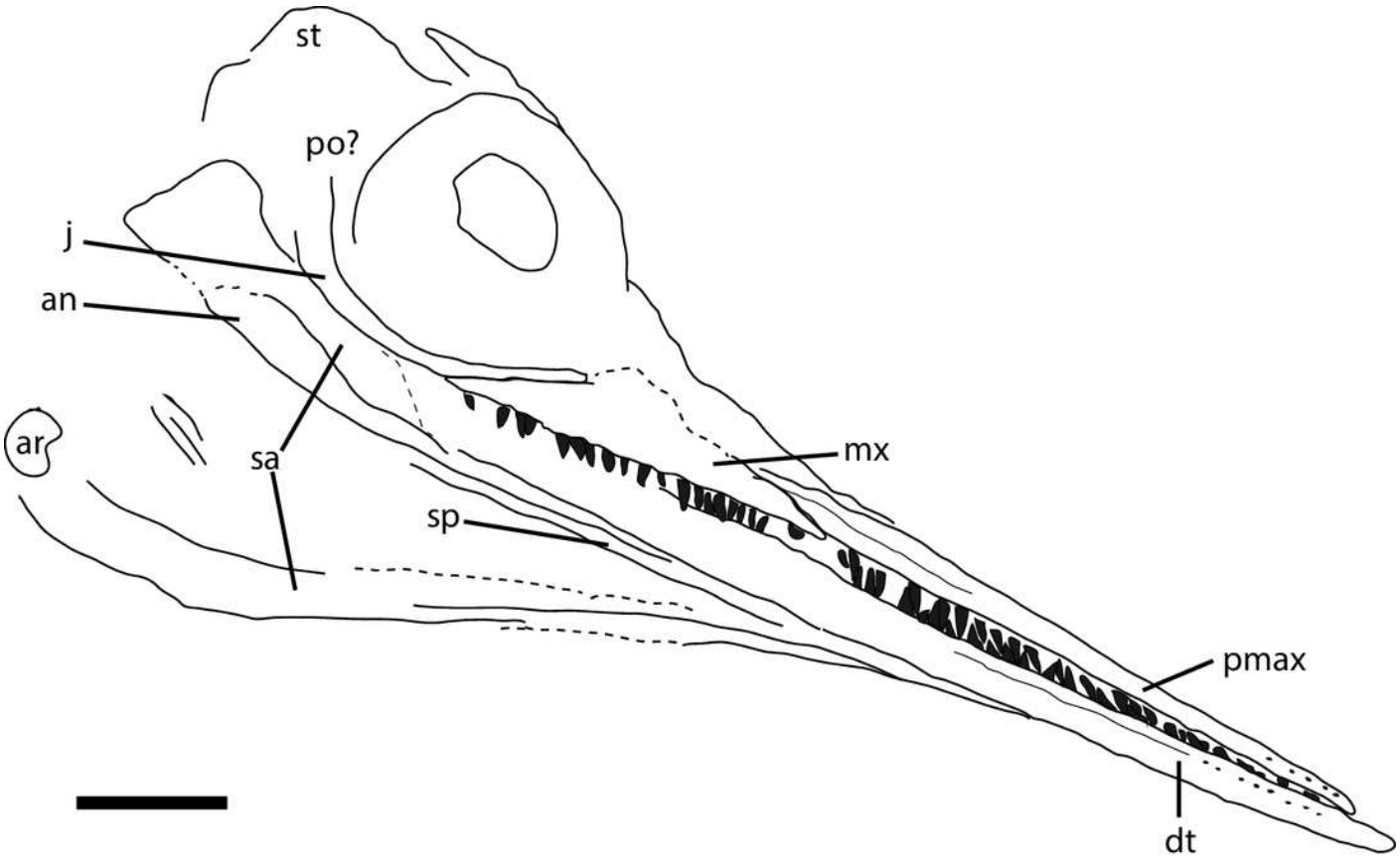

Figure 6

Selected pictures of Late Jurassic *Aegirosaurus* sp. (JME-SOS-08369) from Eichstätt-Blumenberg, Germany.

(A) Posterior portion of skull in UV light in posterior-lateral view with type I and II soft tissue. **(B)** Dorsal outline of specimen with type I soft tissue in UV light. **(C)** Anterior portion of the abdomen in regular light. **(D)** Posterior portion of the abdomen in UV light with type II soft tissue. **(E)** Posterior portion of vertebral column and caudal fin in regular light with type I and II soft tissue. Rectangle shows the area where samples for XRD and EDS analyses were taken. **(F)** Caudal fin in UV light with type I and II soft tissue. All scale bars 5 cm.

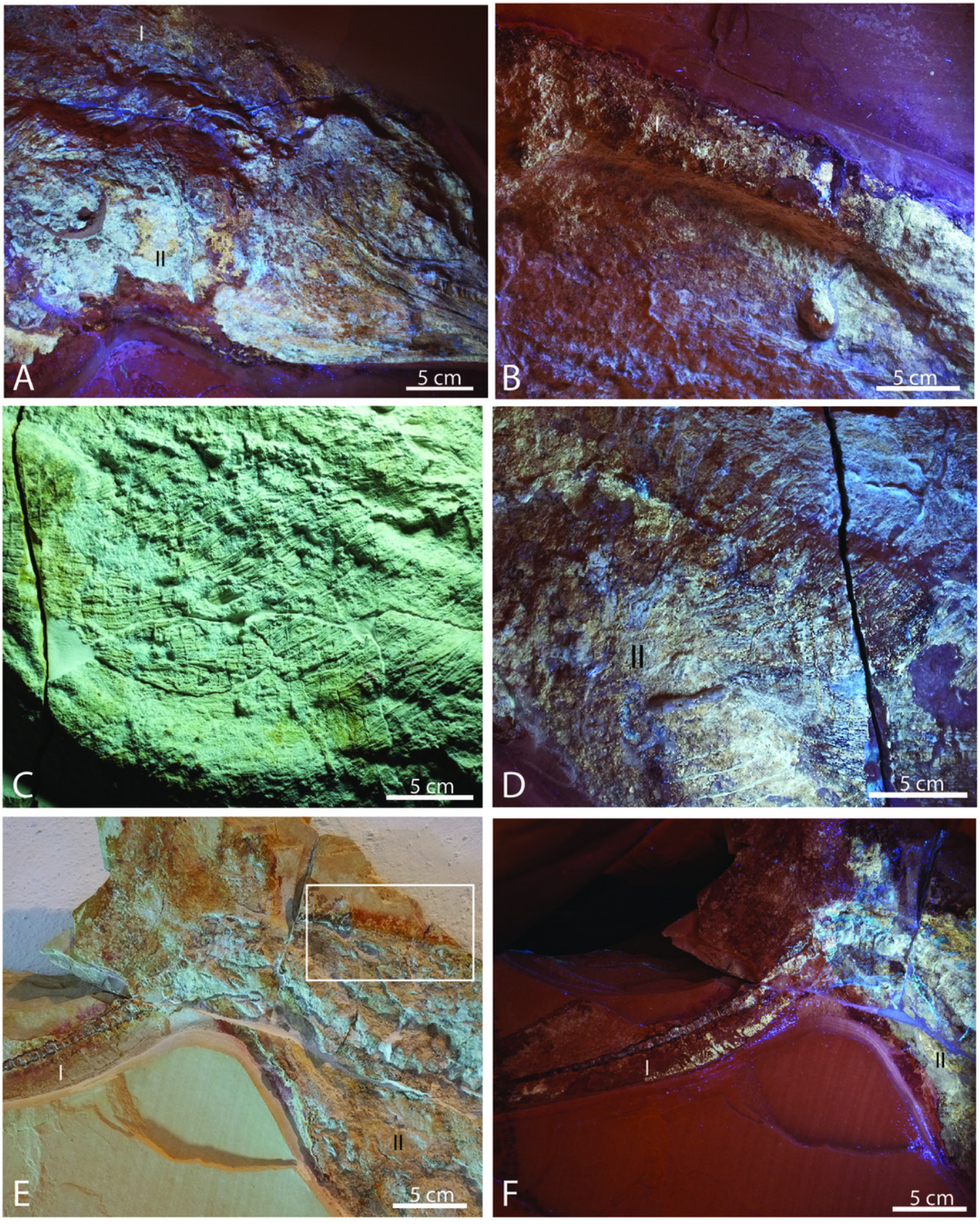
I
II
A
5 cm
I
B
5 cm
C
5 cm
II
D
5 cm
I
II
E
5 cm
I
II
F
5 cm

Figure 7

SEM-EDS of Late Jurassic *Aegirosaurus* sp. (sample JME-SOS-08369-B2) from Eichstätt-Blumenberg, Germany.

(A) SEM back-scatter image where the circle shows the area from which the EDS analysis of (**B)** is taken. (**C)-(F)** are element maps corresponding to A, showing the sharp boundary between the fossil (rich in P in the form of apatite) and the surrounding matrix free of apatite. Scale bar is 100 µm for all images.

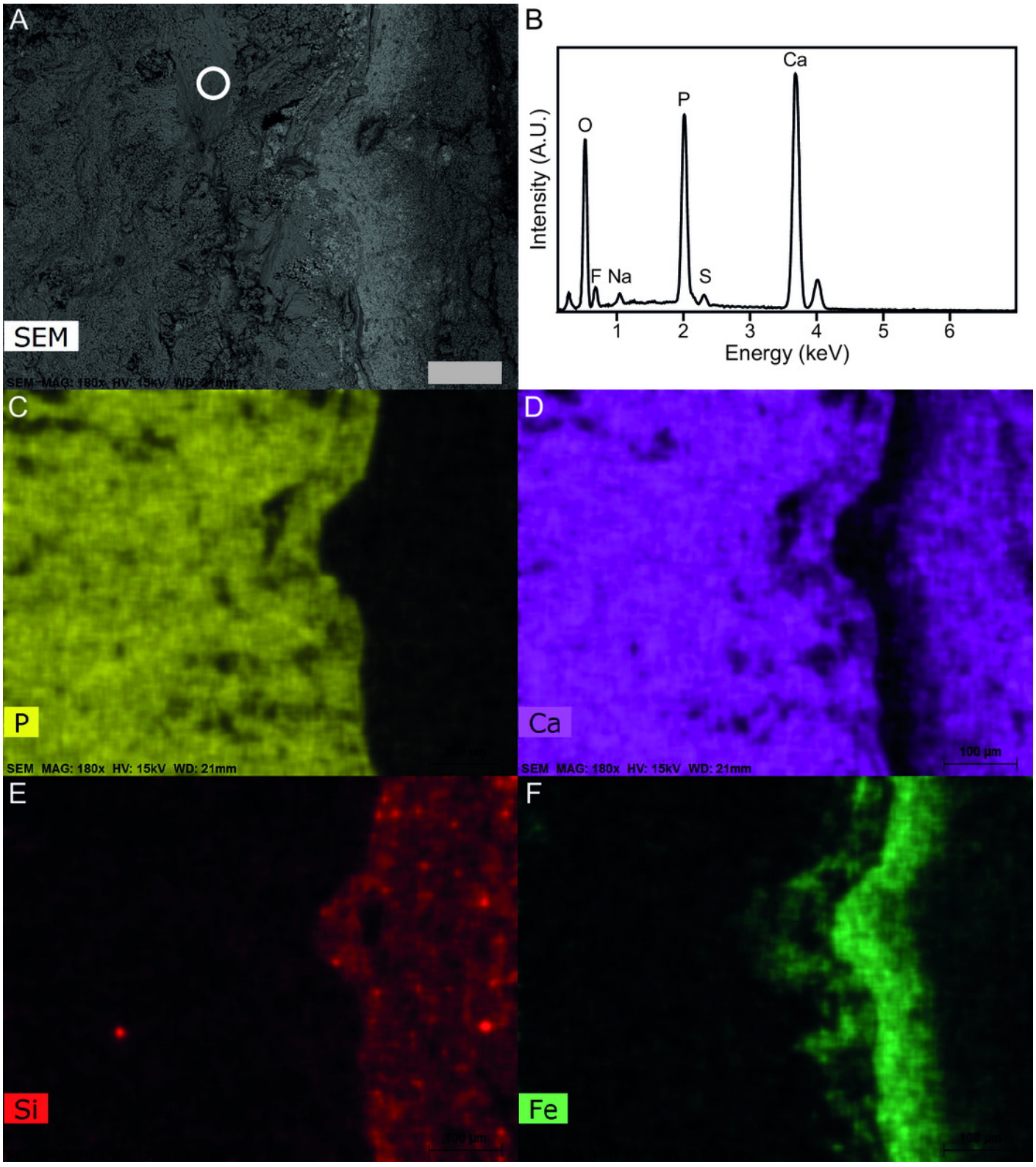
A
O
SEM
SEM MAG: 180x HV: 15kV WD: 21mm
B
Ca
P
O
F Na
S
Intensity (A.U.)
1
2
3
4
5
6
Energy (keV)
C
P
SEM MAG: 180x HV: 15kV WD: 21mm
D
Ca
SEM MAG: 180x HV: 15kV WD: 21mm
100 µm
E
Si
F
Fe